

Original Research Paper

Study of Mutual Coupling of Typical Commercial UHF RFID Tags in a High-Density Environment

¹Gbamélé Konan Fernand, ¹Akpata Edouard, ¹Assamoi Claude Daniel, ¹Gnamele N'tcho Assoukpou Jean, ¹Youan Bi Tra Jean Claude, ¹Ouattara Yelakan Berenger and ²Konan Kouassi Fransisco

¹Laboratory of Technology of the University Félix Houphouët Boigny, Abidjan-Ivory Coast, Côte d'Ivoire

²Higher Normal School, Abidjan-Ivory Coast, Côte d'Ivoire

Article history

Received: 20-08-2022

Revised: 14-09-2022

Accepted: 17-09-2022

Corresponding Author:

Gbamélé Konan Fernand
Laboratory of Technology of
the University Félix Houphouët
Boigny, Abidjan-Ivory Coast
Email: kgbamel@gmail.com

Abstract: In the context of high-density passive UHF (Ultra High Frequency) RFID (Radio Frequency Identification) tag technology, the problem of mutual coupling has to be taken into account as one of the performance criteria of UHF RFID systems. In practical applications, mutual coupling changes the intrinsic parameters of the antennas attached to these tags, i.e., the impedance matching of the antenna and the chip and the radiation pattern. The objective of this study is to study the performance of some commercial tag prototypes by their level of sensitivity to mutual coupling. The 3D initialization model of the Printed Dipole, Printed T-Match, and Printed Meander tags were used to directly extract the mutual impedance values in various scenarios by the ANSYS HFSS software and compare them with the MATLAB software. The simulated results show the effectiveness of this study in obtaining a clear understanding of the performance of the tags. These results open new perspectives on the study of mutual tag-to-tag coupling for research and will help users to make better decisions in the choice of UHF RFID tags for the radio frequency identification of products.

Keywords: UHF RFID Tags, Mutual Coupling, Mutual Impedance, Printed Dipole, T-Match, Printed Meander Dipole

Introduction

Radiofrequency identification systems, or RFID, clearly represent one of the tools that enable the industry, as evidenced by the recent literature (De Oliveira *et al.*, 2019). Their recent technological improvements and the reasonably limited cost of the required infrastructure offer researchers and practitioners a good tool to design and realize interesting applications (Zhong *et al.*, 2017).

Ultra-High Frequency Radio Frequency Identification (UHF RFID) plays a role in tracking and identifying goods and people. In some applications such as traceability (Wang *et al.*, 2022), logistics and supply chain management (Nayak, 2019), or an application in the apparel industry (Nayak *et al.*, 2019), the density of UHF RFID tags is high.

UHF RFID tags are generally expected to dominate the near-field application market in the coming decades (Jaakkola *et al.*, 2019). On the other hand, the research on short-range communication between passive UHF RFID tags (Yao *et al.*, 2016) and wireless power transfer between tags (Yao *et al.*, 2017) has opened up new application opportunities in the UHF band. The communication performance of UHF RFID systems depends on the relative position of the tags (Nikitin and Rao, 2006).

In addition, the proximity of the tags creates significant Electromagnetic (EM) coupling between their respective antennas. As a result, antenna characteristics such as radiation or input impedance are modified. These changes have an impact on the communication performance between the reader and the tags since the difference between the modulation states and implicitly the modulation depth is impacted (Marrocco and Caizzone, 2012). Therefore, a better understanding of the principles of wireless propagation and the coupling between the tag antennas is needed.

Several existing systems have proven that mutual coupling generates considerable interference with the collected phase angle of RFID tags, which degrades the localization performance (Ding *et al.*, 2018; Xiao *et al.*, 2017). This context leads to configurations where the tags are strongly coupled. Gbamélé *et al.* (2019), use patch antennas to study the impact of mutual coupling between the antennas. From their study, it is found that the influence of mutual coupling on the mutual coupling capacity when the patches are very close. However, this study is not extended to other tags commonly deployed in RFID applications.

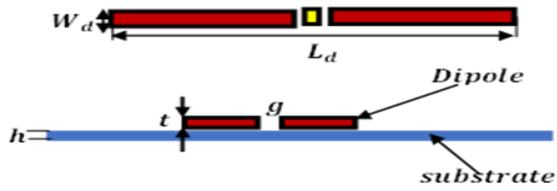


Fig. 1: Standard printed dipole antenna

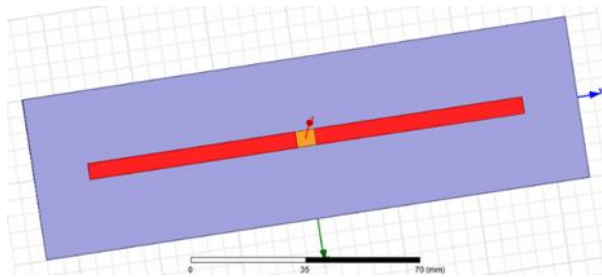


Fig. 2: Differentially fed planar dipole antenna structure used in the simulation

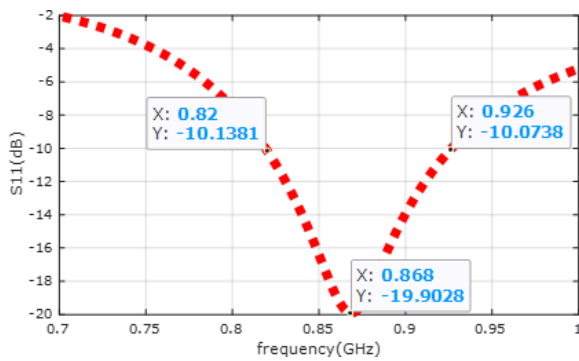


Fig. 3: S₁₁ Simulated reflection coefficients of a planar dipole antenna

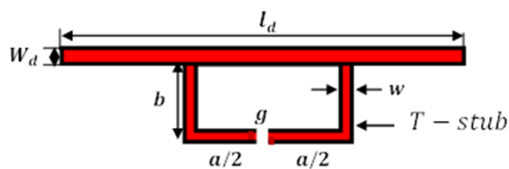


Fig. 4: Structure of the printed T-Match passive UHF RFID tag

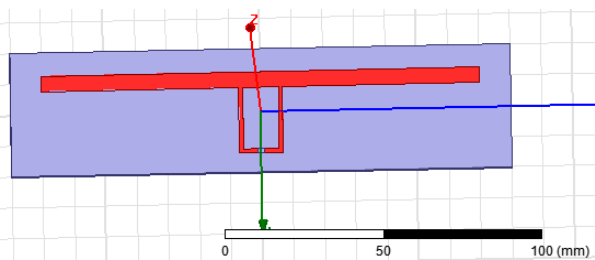


Fig. 5: T-Match half-wave planar dipole antenna under HFSS

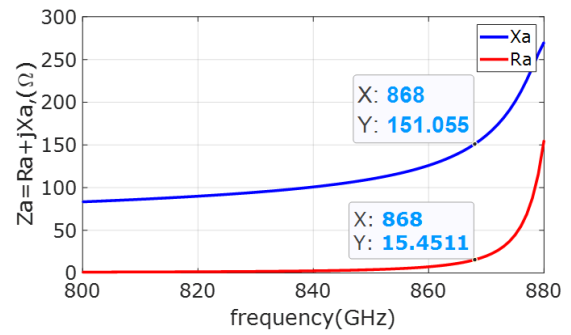


Fig. 6: Input impedance of the simulated antenna as a function of frequency

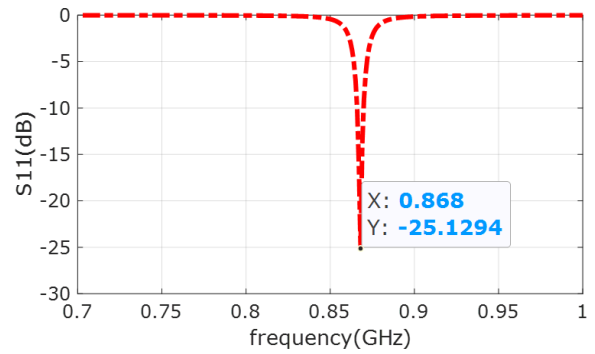


Fig. 7: S₁₁. Simulated reflection coefficients of a planar T-Match dipole antenna

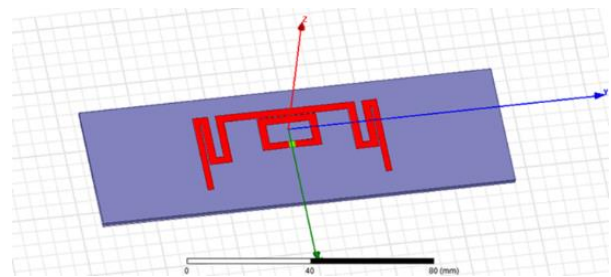


Fig. 8: Proposed meander dipole antenna

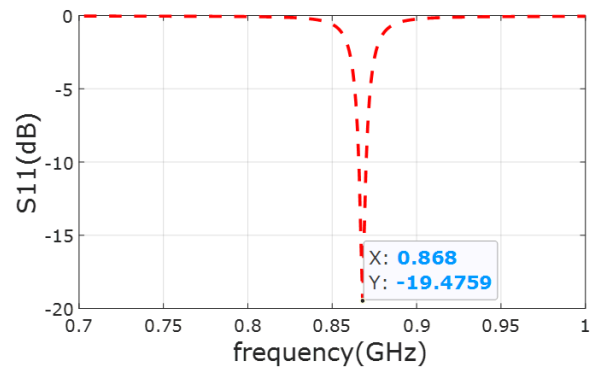


Fig. 9: Reflection coefficient S₁₁ of the proposed meander tag under HFSS

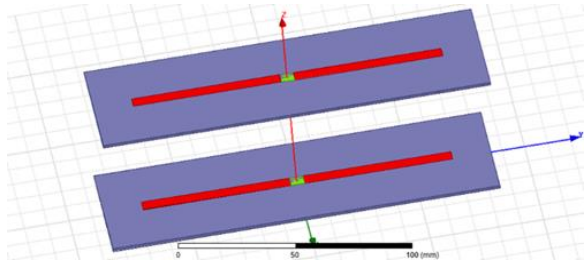


Fig. 10: Coupling between two parallel planar dipoles for a side-by-side configuration in the vertical plane

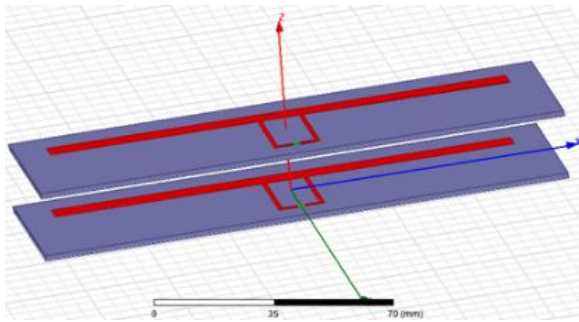


Fig. 11: Coupling between two parallel T-match planar dipoles for a side-by-side configuration in the vertical plane

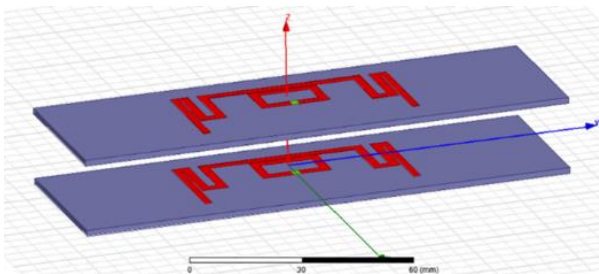


Fig. 12: Coupling between two parallel planar meander dipoles for a side-by-side configuration in the vertical plane

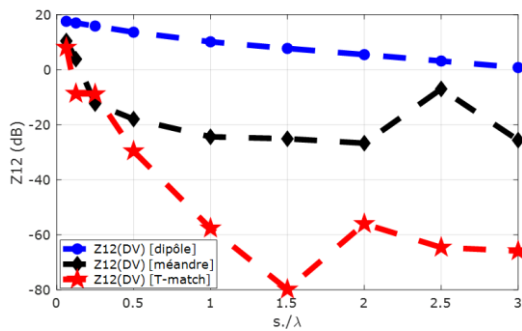


Fig. 13: Mutual impedance Z_{12} of commercial Tags as a function of s/λ in a vertical configuration

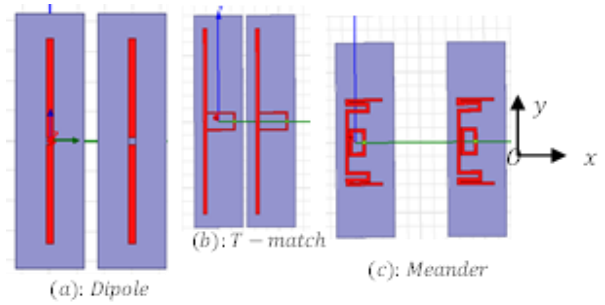


Fig. 14: Side-by-side configurations of mutually coupled printed tags: (a): Dipoles, (b): T-Matches, and (c): Meanders

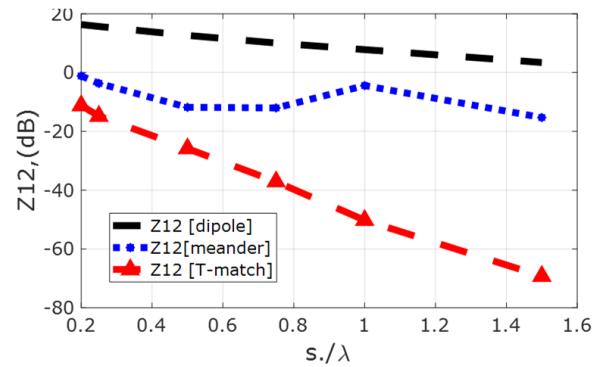


Fig. 15: Mutual impedance Z_{12} of commercial Tags as a function s/λ in a horizontal configuration

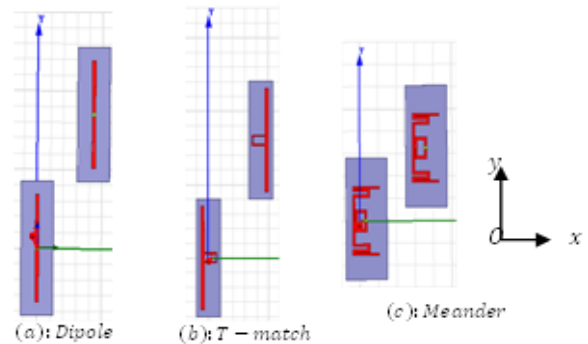


Fig. 16: Parallel -in-echelon configuration of the mutual tag coupling : (a) Dipoles, (b): T-Matches, and (c): Meanders

Table 1. Final dimensions of a planar dipole antenna

Parameters	Value (mm)
Dipole width: W_d	5.0000
Dipole length: L_d	130.0000
Substrate width: W_s	50.0000
Substrate length: L_s	170.0000
Feed point: g	6.0000
Conductor thickness: t	0.0035
Substrate thickness: h	1.6000

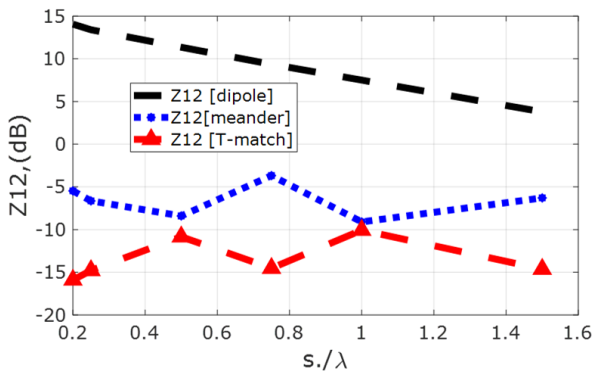


Fig. 17: Mutual impedance Z_{12} of commercial Tags as a function s/λ the parallel -in-echelon configuration

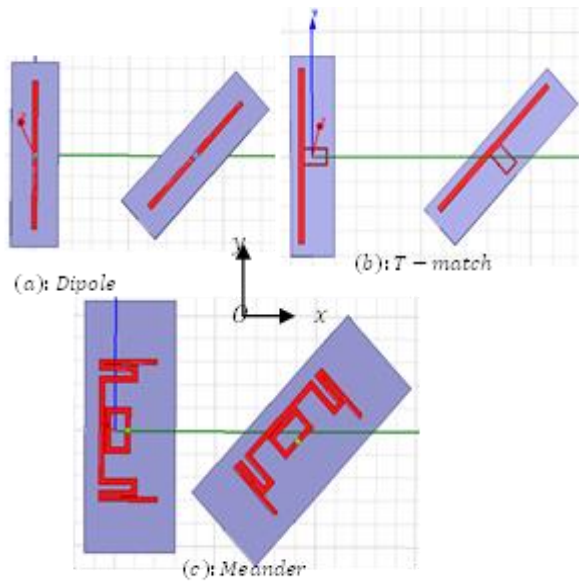


Fig. 18: Geometric configuration of the tags spaced and inclined at an angle of $\theta = 45^\circ$

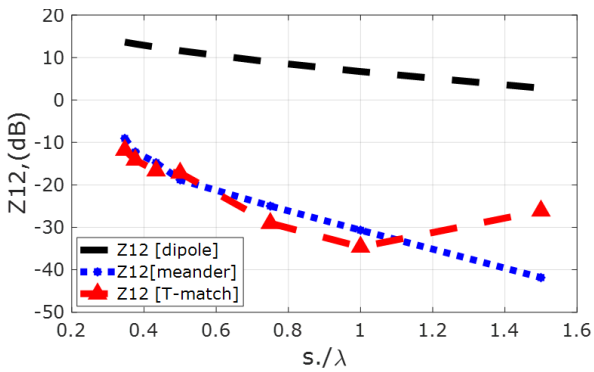


Fig. 19: Mutual impedance Z_{12} of commercial Tags as a function s/λ in the arbitrary configuration

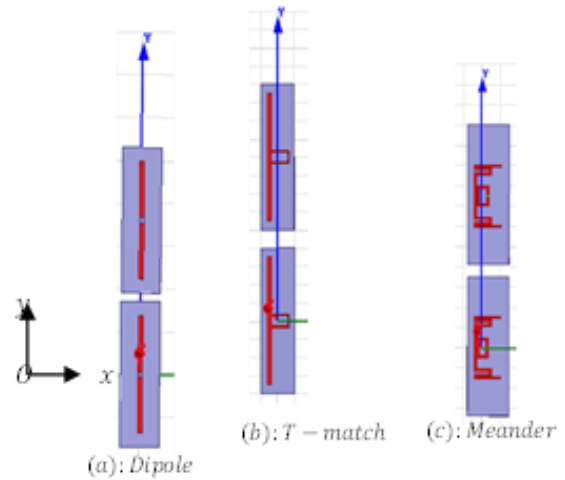


Fig. 20: Mutual coupling in the collinear configuration between the tags: (a): Dipoles, (b): T-Matches, and (c): Meanders

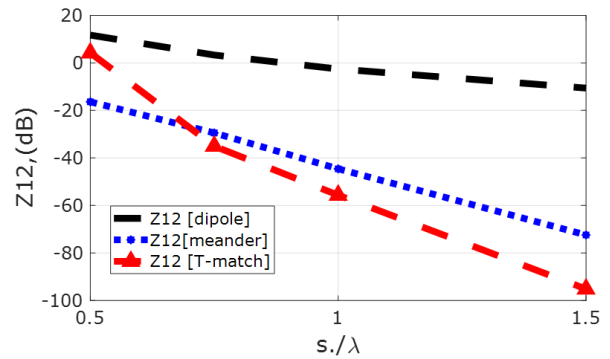


Fig. 21: Mutual impedance Z_{12} of commercial Tags as a function s/λ in the collinear configuration.

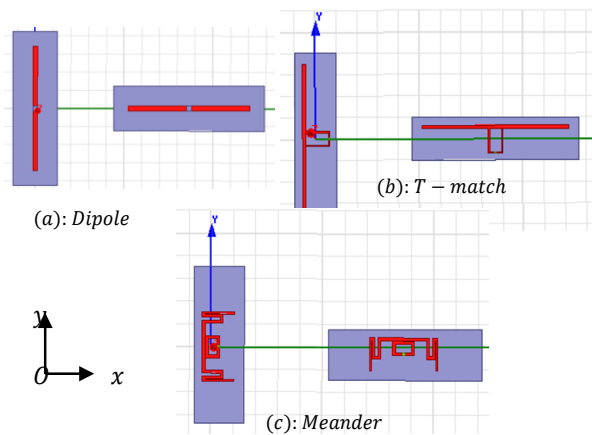


Fig. 22: Mutual coupling in a perpendicular tag configuration: (a): Dipoles, (b): T-Matches, and (c): Meanders

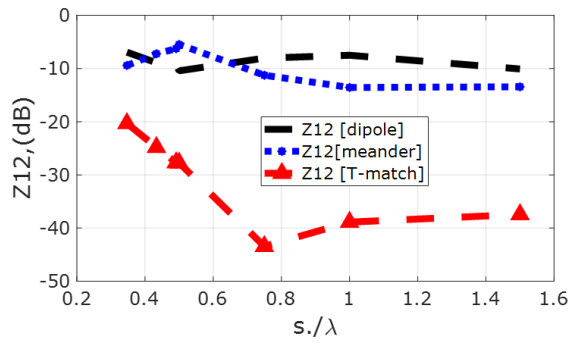


Fig. 23: Mutual impedance Z_{12} of commercial Tags as a function s/λ in the perpendicular configuration

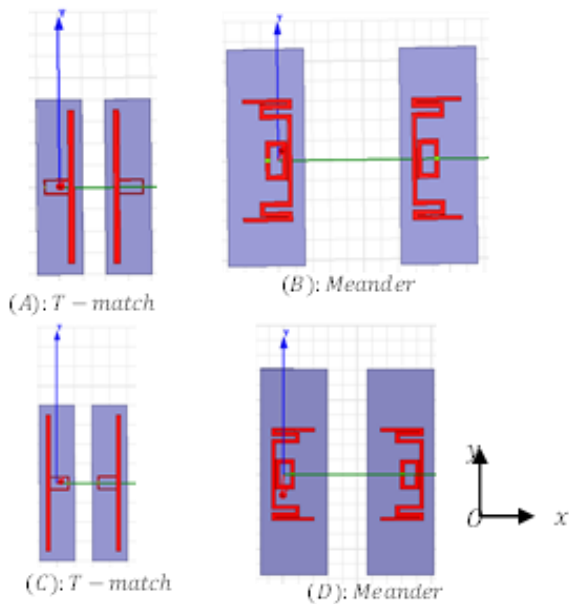


Fig. 24: Mutual coupling in side-by-side tag configuration: (A and C): T-Matches and (B and D): Meanders

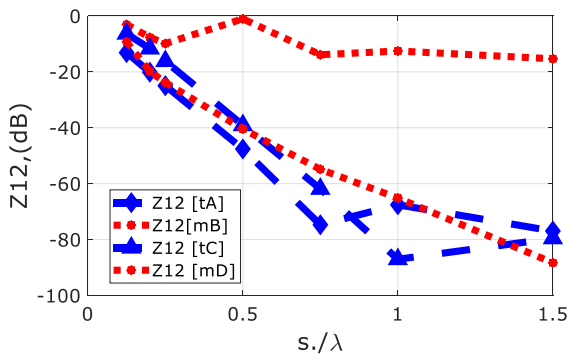


Fig. 25: Mutual impedance Z_{12} of the commercial Tags as a function of s/λ in the face-to-face and back-to-back tag configuration

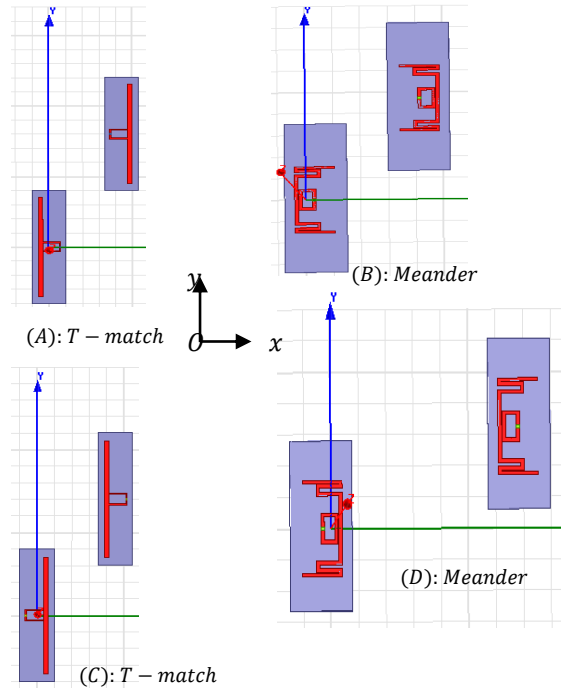


Fig. 26: Parallel -in-echelon configuration of the mutual tag coupling: (A and C): T-Matches and (B and D): Meanders

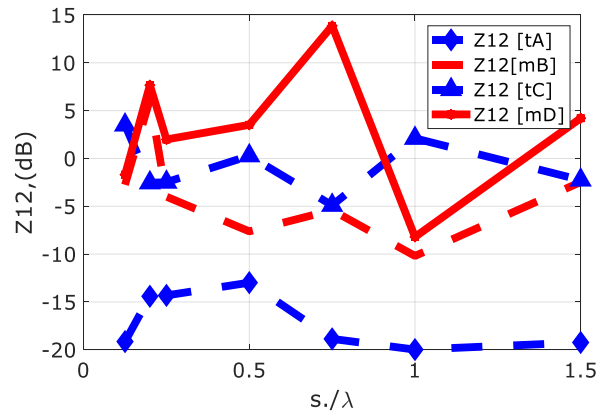


Fig. 27: Mutual impedance Z_{12} of the commercial Tags as a function of s/λ in the parallel-in-echelon, face-to-face, and back-to-back tag configuration

Table 2: Parameters of the printed T-Match dipole

Parameters	Value (mm)
Dipole width: W_d	5.0000
Dipole length: L_d	130.0000
Substrate width: W_s	50.0000
Substrate length: L_s	170.0000
Feed point: g	6.0000
Conductor thickness: t	0.0035
Substrate thickness: h	1.6000

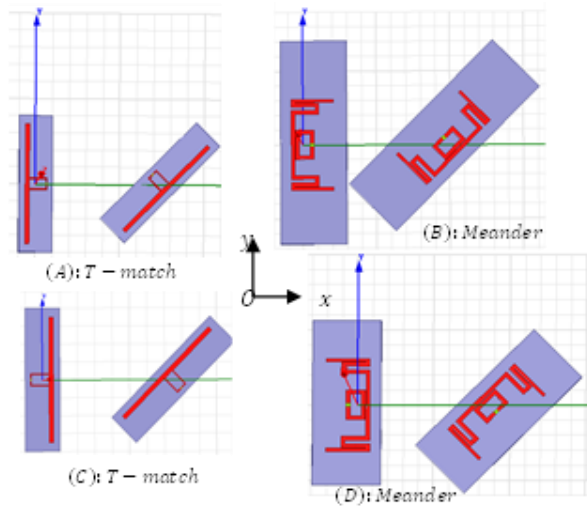


Fig. 28: Geometric configuration of the coupled tags spaced and inclined at an angle of $\theta = 45^\circ$: (A and C): T-Matches and (B and D): Meanders

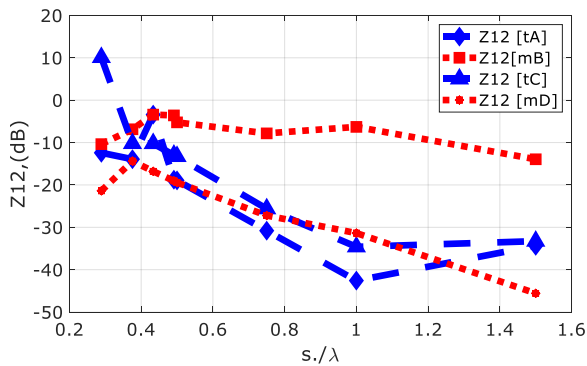


Fig. 29: Mutual impedance Z_{12} of the commercial tags as a function of s/λ in the arbitrary, face-to-face, and back-to-back configuration

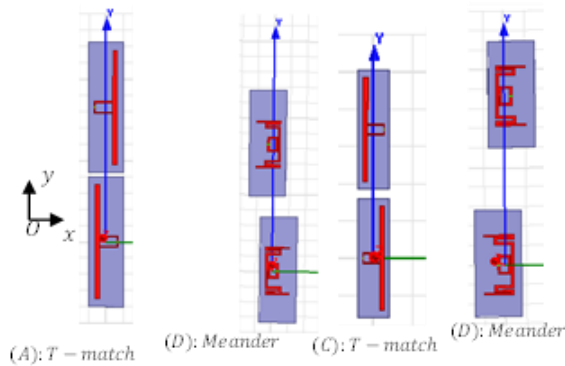


Fig. 30: Collinear configuration of the mutual coupling tags: (A and C): T-Matches and (B and D): Meanders

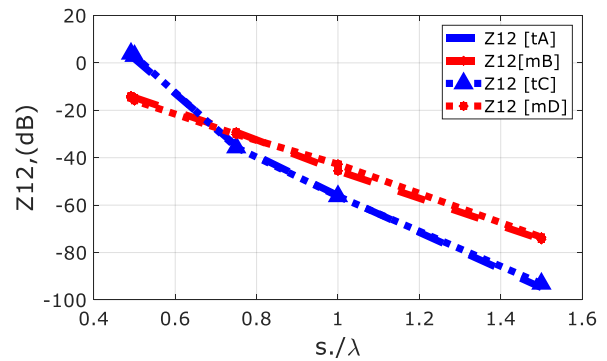


Fig. 31: Mutual impedance Z_{12} of commercial tags as a function of s/λ in collinear, face-to-face, and back-to-back configuration

Table 3. Parameters of the printed meander dipole

Parameters	Value (mm)
Meander width: W_m	20.5
Meander length: L_m	61.0
Substrate width: W_s	24.5
Substrate length: L_s	94.0
Feed point: g	2.0
Loop length:	19.6
Loop width: b	10.0
Loop distance - Meander: dipole	3.0
Loop thickness: w	2.5

With the prevalence of UHF RFID implementation, tag performance analysis is an important factor to study (COSTA, 2005). The far-field performance of the tags does not depend on the position and orientation, unlike the near-field, they are considerably reduced due to a strong mutual coupling between them (Catarinucci *et al.*, 2011) (Chen and Chen, 2009). Therefore, the mutual coupling of UHF RFID tags must be taken into account for optimal deployment of RFID systems. The relative position and orientation of the tags are studied by considering Short Circuit (SC) and Open Circuit (OC) modes (Lassouaoui *et al.*, 2021). But this study has limitations in practice where all UHF tags are illuminated by the RF field in the reader interrogation zone. Moreover, not all configurations are analyzed as presented in this manuscript.

The objective is to evaluate the performance of some basic commercial RFID tag designs through the effect of coupling between tags. Throughout the presented preliminary work, simulations have been performed using typical commercial passive UHF tag designs of three different most commercialized models. The simulations are performed on commercial tags (printed dipoles, printed planar T-Match dipoles, and printed meander dipoles) to predict their "group behavior" in a high-density deployment context. The impact of mutual coupling on the surrounding RFID tags is examined. The commercial software ANSYS HFSS 2015 (High-Frequency Structure Simulator) is

used to extract the mutual impedance Z_{ij} in different tag configurations. Based on the simulation data, MATLAB 2020b (Matrix Laboratory) software is used to compare the impact of mutual coupling on commercial passive UHF RFID tags (printed dipole, printed T-match, and sinuous dipole with inductive structure) to determine which one is the least sensitive to mutual coupling in the different configurations.

In this study, the simulations, the tags are excited by localized ports each having a feed impedance of 50Ω , the frequency of the simulations in this study is 868 MHz. The antenna elements of the tags are excited simultaneously.

Structure of the Passive RFID UHF Tags used

Design of the Printed UHF RFID Tag

Dipole Antenna

Figure 1 shows the considered structure of a dipole antenna used in radio systems compared to traditional linear antennas due to their advantages (small volume, low weight, and low cost), and they are much more suitable for sensitive applications (mobile receivers, vehicle radio receivers, and RFID tags) (Park *et al.*, 2019). The presented configuration will be used to determine the mutual coupling between the printed dipoles and determine the mutual impedance. The resonant frequency depends on the length and width of the printed dipole antenna. Therefore, to find an optimal design, these two parameters must be carefully analyzed. Figure 1 shows the basic geometry of a standard printed dipole antenna with typical parameters.

The differential-fed planar dipole antenna was designed and Fig. 2 shows the structure. The FR-4 substrate, with a dielectric constant $\epsilon_r = 4.4$, tangential loss $\tan\delta = 0.0019$, and a thickness of 1.6 mm, was used as the substrate due to its wide use in UHF RFID tags. The planar dipole antenna (calculations based on a half-wave dipole antenna) was designed for a resonant frequency of 868 MHz.

Based on the above analysis and due to manufacturing constraints, the final dimensions of the printed dipole are shown in Table 1. Figure 3 shows the S_{11} reflection coefficient of the printed dipole antenna. A reflection coefficient S_{11} of about -20 dB is obtained at a frequency of 868 MHz, with a bandwidth of about 100 MHz.

T-Match Printed Antenna Design for UHF RFID Tag

The antenna whose size is smaller than the resonant (radiation) length has a capacitive input impedance. Therefore, impedance matching must be used in the antenna design, so that the antenna can be matched to the impedance of the highly capacitive chip. T-matching or shunt matching is a commonly used technique for impedance matching. T-matching which

was developed (Uda and Mushiake, 1954) is formed by connecting a dipole of radius w_d and length L_d , to another short dipole of radius w and length ($a \leq L_d$) as shown in Fig. 4. The two dipoles are separated by a distance b shown in Fig. 4. The distribution of current along the two conductors is dependent on the size of the cross-section of the dipole. By adjusting the parameters b , a , and w_d , the antenna impedance can be finely tuned to match the chip impedance. Figure 5 shows the configuration of the proposed tag which is printed on a single-sided FR4 PCB (Printed Circuit Board) substrate having $\epsilon_r = 4.4$, $\tan\delta = 0.0019$, and thickness $h = 1.6$ mm with copper deposition thickness $t = 0.035$ mm. The proposed tag is then simulated using Ansys HFSS commercial electromagnetics software in Fig. 5. The geometrical parameters of the HFSS modeled antenna are presented in Table 2. The performance of the proposed tag antenna is then evaluated.

The tag matches an integrated circuit of the Alien Higgs-2 Chip, An EPC Global Class-1 Gen-2 ISO/IEC 18000-6C UHF RFID IC (Alien, 2008) with an input impedance of $(15-j151) \Omega$ and a parallel equivalent resistance $R_p = 1500 \Omega$ and a parallel capacitance $C_p = 1$, $2pF$ in the 860-960 MHz frequency band is shown in Fig. 6. The designed antenna impedance of $(15.4511+j151.055) \Omega$ is shown in Fig. 6, achieves an upper conjugate match with the given electronic tag chip at 868MHz. The procedure for finding the equivalent circuit parameters is based on the quality factor of the proposed tag antenna taken at $Q_p = 10$.

The reflection coefficient S_{11} is shown in Fig. 7. In Fig. 7, the trace of the return loss S_{11} shows that the antenna is resonant around 868 MHz and the corresponding return loss is -25.1294 dB.

Dipole Structure of the Meander Antenna of the Printed UHF RFID Tag

Impedance matching of passive antennas of UHF RFID tags can also be achieved by using a small inductive coupling loop placed close to the radiating body (Son and Pyo, 2005). In this case, the antenna consists of a small rectangular loop, the two terminals of which are connected directly to the chip and a radiating body; the two elements are inductively coupled, and the strength of the coupling is controlled by the distance between the loop and the radiating element. Thus, the design of tag antennas for passive UHF RFID systems is particularly challenging because impedance matching is not targeted at 50Ω transmission lines. The design goal is to match the antenna impedance ($Z_a = R_a + j X_a$) to the impedance of the attached chip, which typically has a highly capacitive reactance. To compensate for the high capacitive reactance, the inductive power supply structure shown in Fig. 8 is a popular choice. Thus, the structure in Fig. 8 is used to study the validity of the simulation. It consists of a meander dipole antenna and a coupled rectangular loop, on which the chip will be mounted, printed on an FR4 substrate

of thickness $h = 1.6$ mm (dielectric constant $\epsilon_r = 4.4$ and tangent loss $\tan\delta = 0.0019$). The detailed and optimized parameters of the inductive antenna coupled to the meander line shown in Fig. 8 are presented in Table 3. Figure 9 shows the reflection coefficient of the proposed antenna. It can be seen that the reflection coefficient S_{11} is a function of frequency and the -10 dB bandwidth representation. The minimum of S_{11} is centered on the frequency of 868 MHz, the resonant frequency of the antenna. And it can be seen that its value of -19.4226 dB is sufficiently small at this frequency, which confirms the suitability of the proposed antenna. After presenting the design of the three tags commonly used in the basic design of UHF RFID tags, the analysis of the effects of mutual coupling ignored in some literature will be examined in the next section. Indeed, when an array of tags is deployed, the effect of mutual coupling becomes a limiting factor for the detection performance. The inductive coupling of neighboring RFID antennas causes energy transfer between closely spaced tags, which generally affects the mutual impedances and the strength of the signal received at the reader.

Simulations, Results in Analysis, and Discussion of the Mutual Impedance Study for UHF RFID Tags

Network of Coupled UHF RFID Tags

A reader is considered in the center of the coordinate to illuminate the UHF RFID tags. The mutual coupling mechanism in transmit mode is considered in this manuscript, one antenna transmits and another receives electromagnetic waves and vice versa. The mutual coupling, which is a near-field phenomenon, causes a change in the input impedance of the RFID tag, resulting in a non-optimal power transfer to the chip. Thus, in applications where multiple RFIDs need to operate next to each other, mutual coupling needs to be taken into account to obtain an accurate design and performance study. To simplify the analysis of mutual coupling, the Z-parameters are used in the literature (Amado and Fano, 2016; Lui *et al.*, 2009) for an identical two-tag system can be calculated using Eq. 1 for a two-port network:

$$\begin{pmatrix} V_1 \\ V_2 \end{pmatrix} = \begin{bmatrix} Z_{11} & Z_{12} \\ Z_{21} & Z_{22} \end{bmatrix} \begin{pmatrix} I_1 \\ I_2 \end{pmatrix} \quad (1)$$

where:

Z_{11} and Z_{22} : Input impedances of the antenna of tag 1 and tag 2 respectively

Z_{21} and Z_{12} : (Mutual) impedances induced in the circuit of the tag 1 antenna from the tag 2 antenna and the tag 2 antenna from the tag 1 antenna respectively

For N UHF RFID tags, the mutual coupling voltage V_{ij} generated at the i^{th} tag due to the current of the j^{th} tag can be written using Eq. 2:

$$V_{ij} = Z_{ij} I_j \quad (2)$$

where:

Z_{ij} : Mutual impedance between the i^{th} and the j^{th} tag

I_j : Current in the j^{th} tag

In practice, the necessary currents and voltages can be calculated using other numerical procedures such as the Finite Element Method (FEM) used by the HFSS solver (Itoh, 1989). This procedure is used to extract the parameter Z_{12} from the mutual coupling in the different scenarios. Using the numerical model of printed dipole tags, printed T-Matches, and Meandered Dipoles, for different values of the ratio d_{12}/λ where d_{12} is the distance between the tags and λ is the wavelength for the 868 MHz frequency, the mutual impedance of UHF RFID tags can be calculated and they are presented in the rest of this manuscript.

Configuration Vertical

The commercial software ANSYS HFSS 2015 is used to extract the mutual impedance Z_{ij} in the Vertical Displacement (DV) of UHF RFID tags. The simulation results are then examined in MATLAB. The individual tags are excited on ports 1 and 2 with 50 Ω Lumped ports. The configurations of the printed dipoles printed T-Match dipoles and printed meandered dipoles are shown in Fig. 10, 11, and 12 respectively. The impact of mutual coupling is evaluated by varying the ratio s/λ between the tags, where λ is the free space wavelength. The results of the simulation in the vertical configuration are presented in Fig. 13 showing the impact of mutual coupling on the tag groups as a function of the ratio s/λ .

Figure 13 shows the mutual impedance Z_{12} for the tags: Dipole/dipole, meander/meander, and T-match/T-match. All curves decrease rapidly with the ratio s/λ . The curves for the T-match tag and the meander dipole show lower mutual impedance values than the conventional planar dipole. The T-Match label would be best suited for high bay deployments due to its low sensitivity to coupling in this configuration.

Side-by-Side Configuration

In this section, the objective is to model by simulations the coupling of passive UHF RFID tags based on the mutual impedance of identical coupled tags regardless of their relative position. For this purpose, the tag antennas are assumed to be printed dipole antennas, printed T-Match antennas, and meandered dipole antennas, as shown in Fig. 14. Assuming parallel tags in a side-by-side configuration at a distance d_{12} in the xOy plane, Fig. 15 shows the mutual impedance Z_{12} as a function of the distance d_{12} between the tags. The coupling effect in terms of mutual impedance is greatest for short distances and gradually decreases with increasing distance as shown in Fig. 15. Figure 15 shows the results obtained. We can see that the printed T-Match tag has a low level of mutual coupling, and is,

therefore, less sensitive to mutual coupling in the "side-by-side" configuration.

Parallel-in-Echelon Configuration

Figure 16 shows the couplings of the printed dipole, printed T-Match, and printed meander tags in step configuration for different distances between tags ranging from 0λ to 1.5λ , respectively. The height of tag 2 is taken at $h = Ls$. The comparison of the evolution of the mutual impedance Z_{ij} as a function of the distance between the tags obtained by simulation with HFSS. Figure 17 shows the results obtained by simulating the evolution of the mutual impedance as a function of the distance d_{12} for three types of passive UHF RFID tags. In the parallel step configuration, the printed dipole tag shows a much stronger coupling than the printed T-Match and meander dipoles. It can be seen that the printed T-Match tag has low mutual coupling, so it is less sensitive to mutual coupling in the parallel-in-echelon configuration.

Arbitrary Configuration

In the arbitrary configuration shown in Fig. 18, the first tag is aligned on the y-axis and the second tag is tilted by an angle θ concerning this axis. To avoid an intersection between the two tags, a minimum distance is set according to the widths of the substrate ends between the two tags. As illustrated in Fig. 18, the tags are placed in close proximity, and the angle of inclination $\theta = 45^\circ$ of the second tag for the y-axis. The distance between the two tags varies between the ends of the tags up to 1.5λ . Under these considerations, the mutual impedance can be calculated using HFSS. Figure 19 shows the simulation results for the parallel step arrangement. In this arrangement, the printed dipole tag shows a much stronger coupling compared to the other two tags. The curves of the T-Match and Meander tags show an almost similar evolution up to 0.5λ . From 0.5λ to λ , the printed T-Match tag shows a weak coupling compared to the meandered dipole tag.

Collinear Configuration

Figure 20 shows the tags in the collinear configuration. The tags are aligned along the y-axis and we fix the center of tag 2 along the y-axis.

The evolution of the mutual impedance as a function of the distance d_{12} between the two tags along the y-axis was obtained by numerical simulation with HFSS.

From the results obtained in Fig. 21, the printed dipole tag always shows high coupling. The meandered dipole tag exhibits low mutual coupling compared to the printed T-match tag for $d_{12} \leq 0.5\lambda$. For $0.5 \leq d_{12} \leq \lambda$, the T-match dipole exhibits low mutual coupling in the collinear configuration.

Perpendicular Configuration of Passives UHF RFID Tags

Figure 22 shows the mutual coupling of passive UHF RFID tags in a perpendicular configuration. One tag is placed along the y-axis and the second is placed along the x-axis. The reference of the distance between the tags is taken from the ends of the different tags. The comparison of the evolution of the mutual impedance as a function of the distance d_{12} between the tags is obtained numerically with HFSS. Figure 23 shows the simulation results. According to the simulation results obtained, the mutual impedance curves decrease as the distance d_{12} increases. It is important to note that the printed dipole tag has a high coupling compared to both tags. The T-Match is less sensitive to coupling and is therefore suitable for this type of deployment. In the following section, the effect of mutual coupling of commercial printed T-Match tags and printed meandered dipoles will be examined in different scenarios.

Face-to-Face and Back-to-Back Tag Configuration

Side-by-Side Configuration

In this side-by-side configuration shown in Fig. 24, the tags are placed face to face and back-to-back. The effect of mutual coupling between the tags is determined by varying the distance d_{12} between adjacent tags and showing acceptable isolation between adjacent tags with the HFSS software. Figure 25 shows a comparison of the mutual impedances obtained using MATLAB. It can be seen from this comparison that the tags in configurations A (tA: T-match in configuration A) and C (tC: T-match in configuration C) have a lower level of mutual coupling than the tags in configurations B (mB: Meander in configuration B) and D (mD: Meander in configuration D).

Parallel-in-Echelon Configuration

Figure 26 shows two tags in a step configuration. The height of tag 2 is fixed at $h = Ls$. The evolution of the mutual impedance as a function of the separation distance d_{12} of the tags is realized. In this step configuration shown in Fig. 26, the tags are placed face to face and back-to-back. Figure 27 compares the mutual impedances obtained. The mutual coupling in configuration A of a tag is low compared to that in configuration B; at the same time, the mutual coupling in configuration C of a tag is low compared to that in configuration D.

Arbitrary Configuration

In the arbitrary face-to-face and back-to-back configuration of Fig. 28, as before, the left tag is aligned along the y-axis and the second tag is tilted at an angle θ to the y-axis. To avoid an intersection between the two tags, a minimum distance is set based on the widths of the

substrate ends between the two tags. As shown in Fig. 28, the tags (T-matches and Meanders) are placed in close proximity and the angle of inclination $\theta = 45^\circ$ of the second tag to the y-axis. The distance between the two tags varies between the ends of the tags up to 1.5λ .

Figure 29 shows the evolution of the mutual impedance Z_{12} as a function of the ratio s/λ . Although the mutual coupling curves of all tag configurations decrease with increasing distance d_{12} , the mutual coupling of the tags in configurations A and C where the T-Matches are printed is low compared to configurations B.

Opposite Tags in Collinear Configuration

Figure 30 shows tags in a collinear and opposite configuration. The tags are aligned along the y-axis. The comparison of the evolution of the mutual impedance as a function of the distance d_{12} between the two tags coupled along the y-axis was obtained by numerical simulation.

In Fig. 31, the influence of the distance between the tags on the mutual coupling is studied. It is observed that the coupling between the tags in the different configurations decreases as the distance d_{12} increases. Thus, the level of mutual coupling in cases A and C (blue curves for T-Matches) is higher when $d_{12} < 0.5 \lambda$ than in cases B and D (red curves for meandered dipoles) and lower when $0.5 \lambda < d_{12} < \lambda$ compared to cases B and D.

Conclusion

In the context of new Passive UHF RFID systems in a dense deployment, this study studied the impact of mutual coupling between tags as a function of their relative position and orientation in different configurations. The mutual coupling, which can be considered as an evaluation parameter for RFID systems, strongly impacts the self-impedances and the radiation pattern and thus reader-tag switching.

These results show that Passive UHF RFID systems present unstable performances depending on the considered configurations, which is a limiting factor in practice. Future applications will have to take this aspect into account.

This study allowed us to understand the behavior of tags in a dense environment. The T-match tag is weakly coupled in almost all configurations. It has an advantage over the two tags chosen for the study. But it has a disadvantage compared to the meandered dipole which has a small size. The meandered dipole follows the T-match tag in classification. Therefore, it would be ideal for various applications in RFID systems.

The study presented in this study predicts the group behavior among UHF RFID tags in the market, which can help users to make a good choice based on their usage. Based on the surrounding tag analysis methodology developed in this study, the comparative study of group behavior of different existing tag designs in UHF RFID systems is a first.

For future work, studies will be carried out on more complex tags to make the study more general and guide users to make judicious choices, and contribute to increasing the performance of UHF RFID systems in a context of high tag density.

Acknowledgment

The researchers would like to express their great appreciation to the Technology Laboratory of the University of Félix Houphouët Boigny, for the support provided to conduct this research study.

Author's Contributions

Gbamélé Konan Fernand: Contributed on the original ideas of the research, data collection, analysis and interpretation and manuscript writing.

Akpata Edouard, Gnamele N'tcho Assoukpou Jean and Youan Bi Tra Jean Claude: Designed the MATLAB programs. Wrote most of the paper.

Assamoi Claude Daniel and Ouattara Yelakan Berenger: Contribution to the design of tags in HFSS. Contributed to the writing of the article.

Konan Kouassi Fransisco: Designed the research plan and supervised its execution.

Ethics

This manuscript is the original work of the authors and has not been previously published elsewhere. The authors confirm that they have read and approved this study and that no ethical issues are involved.

References

- Alien. (2008, July). Alien Higgs-2 Chip, An EPC Global Class-1 Gen-2 ISO/IEC 18000-6C UHF RFID IC. <https://www.alientechnology.com>
- Amado, J., & Fano, G. (2016, November). Antenna coupling model in receiving mode. In *2016 IEEE Global Electromagnetic Compatibility Conference (GEMCCON)* (pp. 1-5). IEEE. <https://doi.org/10.1109/GEMCCON.2016.7797321>
- Catarinucci, L., Colella, R., De Blasi, M., Patrono, L., & Tarricone, L. (2011). High-performance UHF RFID tags for item level tracing systems in critical supply chains. *Current Trends and Challenges in RFID*, 10, 187-208.
- Chen, Y. S., & Chen, S. Y. (2009, June). Analysis of antenna coupling in near-field RFID systems. In *2009 IEEE Antennas and Propagation Society International Symposium* (pp. 1-4). IEEE. <https://doi.org/10.1109/APS.2009.5172382>
- Costa, L. R. (2015, October). UHF RFID tags in a controlled environment: Anechoic chamber case. In *2015 IEEE Brasil RFID* (pp. 1-5). IEEE. <https://doi.org/10.1109/BrasilRFID.2015.7523836>

- de Oliveira, A. O., Oliveira, H. L. S., Gomes, C. F. S., & Ribeiro, P. C. C. (2019). Quantitative analysis of RFID' publications from 2006 to 2016. *International Journal of Information Management*, 48, 185-192. <https://doi.org/10.1016/j.ijinfomgt.2019.02.001>
- Ding, H., Han, J., Qian, C., Xiao, F., Wang, G., Yang, N., ... & Xiao, J. (2018, April). Trio: Utilizing tag interference for refined localization of passive RFID. *In IEEE INFOCOM 2018-IEEE Conference on Computer Communications* (pp. 828-836). IEEE <https://doi.org/10.1109/INFOCOM.2018.8486313>
- Gbamélé, F. K., Ouattara, Y. B., Siaka, F., & Doumbia, I. (2019, August) « Study of the coupling between UHF RFID tags with high degree of confinement », *ijias*, pp. 401-409. <http://www.ijias.issr-journals.org/>
- Itoh, T. (1989). Numerical techniques for microwave and millimeter-wave passive structures. *Wiley-Interscience*.
- Jaakkola, K., Sandberg, H., Lahti, M., & Ermolov, V. (2019). Near-Field UHF RFID transponder with a screen-printed graphene antenna. *IEEE Transactions on Components, Packaging and Manufacturing Technology*, 9(4), 616-623. <https://doi.org/10.1109/TCPMT.2019.2902322>
- Lassouaoui, T., Hutu, F., Villemaud, G., & Duroc, Y. (2021, October). Modulation depth enhancement for randomly arranged tags in passive RFID tag to tag communications. *In 2021 IEEE International Conference on RFID Technology and Applications (RFID-TA)* (pp. 116-119). IEEE. <https://doi.org/10.1109/RFID-TA53372.2021.9617243>
- Lui, H. S., Hui, H. T., & Leong, M. S. (2009). A note on the mutual-coupling problems in transmitting and receiving antenna arrays. *IEEE Antennas and Propagation Magazine*, 51(5), 171-176. <https://doi.org/10.1109/MAP.2009.5432083>
- Marrocco, G., & Caizzzone, S. (2012). Electromagnetic models for passive tag-to-tag communications. *IEEE Transactions on Antennas and Propagation*, 60(11), 5381-5389. <https://doi.org/10.1109/TAP.2012.2208087>
- Nayak, R. (2019). Radio Frequency Identification (RFID): Technology and Application in Garment Manufacturing and Supply Chain. *CRC Press*.
- Nayak, R., Akbari, M., & Far, S. M. (2019). Recent sustainable trends in Vietnam's fashion supply chain. *Journal of Cleaner Production*, 225, 291-303. <https://doi.org/10.1016/j.jclepro.2019.03.239>
- Nikitin, P. V., & Rao, K. V. S. (2006, July). Performance limitations of passive UHF RFID systems. *In 2006 IEEE Antennas and Propagation Society International Symposium* (pp. 1011-1014). IEEE. <https://doi.org/10.1109/APS.2006.1710704>
- Park, H., Rehman, A., & Lee, C. (2019) «How to Improve Isolation and Electrical Characteristics of Two RFID Tag Antennas, When They Are Located by an Extremely Small Gap », *The transactions of The Korean Institute of Electrical Engineers*, p, 334-341. <http://doi.org/10.5370/KIEE.2019.68.2.334>
- Son, H. W., & Pyo, C. S. (2005). Design of RFID tag antennas using an inductively coupled feed. *Electronics Letters*, 41(18), 1.
- Uda, S., & Mushiake, Y. (1954). Yagi-Uda Antenna. Research Institute of Electrical Communication, Tohoku University.
- Wang, L., He, Y., & Wu, Z. (2022). Design of a Blockchain-Enabled Traceability System Framework for Food Supply Chains. *Foods*, 11(5), 744. <https://doi.org/10.3390/foods11050744>
- Xiao, F., Wang, Z., Ye, N., Wang, R., & Li, X. Y. (2017). One more tag enables fine-grained RFID localization and tracking. *IEEE/ACM Transactions on Networking*, 26(1), 161-174. <https://doi.org/10.1109/TNET.2017.2766526>
- Yao, Y., Cui, C., Yu, J., & Chen, X. (2016). A meander line UHF RFID reader antenna for near-field applications. *IEEE Transactions on Antennas and Propagation*, 65(1), 82-91. <https://doi.org/10.1109/TAP.2016.2631084>
- Yao, Y., Liang, Y., Yu, J., & Chen, X. (2017). Design of a multipolarized RFID reader antenna for UHF near-field applications. *IEEE Transactions on Antennas and Propagation*, 65(7), 3344-3351. <https://doi.org/10.1109/TAP.2017.2700873>
- Zhong, R. Y., Xu, X., Klotz, E., & Newman, S. T. (2017). Intelligent manufacturing in the context of industry 4.0: A review. *Engineering*, 3(5), 616-630. <https://doi.org/10.1016/J.ENG.2017.05.015>